Application of Two-Phase Spray Cooling for Thermal Management of Electronic Devices

Milan Visaria and Issam Mudawar

***Abstract*—Recent studies provide ample evidence of the effectiveness of two-phase spray cooling at dissipating large heat fluxes from electronic devices. However, those same studies point to the difficulty predicting spray performance, given the large number of parameters that influence spray behavior. This paper provides a complete set of models/correlations that are required for designing an optimum spray cooling system. Several coolants (water, FC-72, FC-77, FC-87 and PF-5052) are used to generate a comprehensive spray-cooling database for different nozzles, flow rates, subcoolings, and orientations. High-speed video motion analysis is used to enhance the understanding of droplet formation and impact on the device's surface, especially near the critical heat flux (CHF) point. A previous CHF correlation for normal sprays is modified for both inclination and subcooling effects. A new user-friendly CHF correlation is recommended which shows excellent predictive capability for the entire database. Also discussed in this paper is a new theoretical scheme for assessing the influence of spray overlap on cooling performance.**

***Index Terms*—Defense electronics, phase change cooling, spray cooling.**

NOMENCLATURE

A	Area measured along test surface.
A'	Area measured along spherical surface.
$Bo*$	Modified boiling number.
c_p	Specific heat at constant pressure.
d_o	Diameter of nozzle orifice.
d_{32}	Sauter mean diameter (SMD).
f_1	Ratio of local to average volumetric flux.
f_2	Ratio of point-based CHF to CHF based on total area (L^2) of test surface.
H	Distance of nozzle orifice from test surface.
h_{fg}	Latent heat of vaporization.
L	Length (and width) of square test surface.
$\dot{N}$	Droplet number density.
P	Pressure.
ΔP	Pressure drop across spray nozzle.
P_W	Total electrical power input to test heater.
Q	Total volumetric flow rate of spray.
$\bar{Q}''$	Mean volumetric flux across impact area of spray.
Q''	Local volumetric flux on test surface.
q''	Heat flux based on total area (L^2) of test surface.
q''_m	CHF based on total area (L^2) of test surface.
$q''_{m,p}$	Local (point-based) CHF at outer edge of spray impact area.
q''_{**}	Dimensionless CHF.
r	Radial distance measured from center of test surface.
R	Radius of impact circle for overlapping sprays.
Re_{d_0}	Reynolds number based on orifice diameter; $\rho_f(2\Delta P/\rho_f)^{1/2}d_o/\mu_f$.
T	Temperature.
T_f	Liquid temperature at nozzle inlet.
T_s	Test surface temperature.
T_{sat}	Saturation temperature based on test chamber pressure.
ΔT_{sub}	Fluid subcooling at nozzle inlet, $T_{\mathrm{sat}} - T_f$.
U_m	Mean droplet velocity.
$\mathrm{We}_{\mathrm{d_0}}$	Weber number based on orifice diameter; $\rho_f(2\Delta P/\rho_f)d_o/\sigma$.

Greek Symbols:

α	Inclination angle between spray axis and normal to test surface.
β	Angle used in uniform point source model.
γ, γ'	Angles used in uniform point source model.
θ	Spray cone angle.
ϕ	Angle used in overlap model.
μ	Viscosity.
ξ	Angle used in overlap model.
ρ	Density.
σ	Surface tension.

Subscripts:

f	Liquid; nozzle inlet.
g	Vapor.
m	Maximum (CHF).
p	Point-based (local).
s	Test surface.
sat	Saturation.
sub	Subcooled.

Manuscript received July 01, 2008; revised November 09, 2008 and November 18, 2008. First published March 16, 2009; current version published November 25, 2009. This work was supported by the Office of Naval Research (ONR). This work was recommended for publication by Associate Editor A. Bhattacharya upon evaluation of the reviewers comments.

The authors are with the Boiling and Two-Phase Flow Laboratory (BTPFL) and Purdue University International Electronic Cooling Alliance (PUIECA), Purdue University, West Lafayette, IN 47907-2088 USA.

Digital Object Identifier 10.1109/TCAPT.2008.2010405

I. Introduction

During the past two decades, many liquid cooling schemes have been suggested for the removal of high heat fluxes from electronic devices. Of those schemes, three have gained the most attention: microchannel, jet-impingement, and spray [1]. Proponents of spray cooling point to several advantages of this cooling scheme: high-flux heat dissipation, low and fairly uniform surface temperature, and ability to provide cooling for a relatively large surface area with a single nozzle. However, while microchannel and jet-impingement cooling lend themselves better to modeling and assessment of cooling performance, spray cooling is far more complex. Much of this complexity is the result of the dependence of spray cooling performance on an unusually large number of parameters, which, in addition to the thermophysical properties of the coolant and heater size, include nozzle type, droplet size and volumetric flux (flow rate per unit area) [2]–[5] and the spatial distribution for both [5]–[8], spray angle [5]–[8], orifice-to-surface distance [6]–[8], and fluid subcooling [5]–[10]. Performance is greatly complicated for inclined sprays [11]–[14] and overlapping sprays [15], [16]. There are also additional practical concerns in implementing spray cooling, such as corrosion and erosion of the intricate interior of spray nozzles, single-point failure as a result of nozzle clogging, and lack of repeatability of droplet hydrodynamics and heat transfer performance for seemingly identical nozzles [17]. The present paper is a culmination of several studies by the authors and coworkers that are aimed at filling the knowledge gap in the understanding of spray cooling.

Not all types of nozzles are recommended for electronics cooling. Atomizers are spray nozzles that utilize a secondary gas stream to aid the droplet breakup and produce small droplets. However, mixing a noncondensible gas with the liquid coolant greatly complicates the coolant flow loop due to the need to separate the gas from the spent coolant, let alone the highly detrimental effects of a noncondensible gas on the performance of the flow loop's condenser. Pressure spray nozzles are preferred for electronics cooling because they use the momentum of the liquid coolant to achieve the droplet breakup. Pressure spray nozzles are classified according to the manner in which they distribute droplets across the surface. Hollow-cone spray nozzles, for example, concentrate most of the droplets near the periphery of the impact circle. On the other hand, full-cone spray nozzles distribute droplets across the entire impact circle; they are therefore preferred for electronics cooling. The present study concerns the cooling performance of full-cone pressure spray nozzles.

The spray's hydrodynamic parameters have significant impact on cooling performance. One key hydrodynamic parameter is droplet diameter, often represented by Sauter mean diameter (d_{32}), which is a measure of the ratio of liquid volume to surface area. Smaller droplets are preferred for their ability to increase the surface area of liquid and, therefore, the liquid impact area with the device's surface. Like all cooling schemes, increasing the volumetric flow rate is the most intuitive means for improving spray-cooling performance. Another important measure of flow rate effects is how the flow rate is distributed across the surface. Volumetric flux Q'' is defined as the flow rate of coolant impacting an infinitesimal area of the surface divided by the same area. This locally defined parameter facilitates the assessment of spatial variations of spray cooling. Volumetric flux is essentially the product of mean droplet velocity U_m, droplet size $\pi d_{32}^3/6$, and droplet number density $\dot{N}$; the latter is the number of droplets impacting the surface locally per unit area per unit time. While both volumetric flux and droplet velocity have the units of velocity (m/s), only the former accounts for the important effects of droplet number density, hence the importance researchers have placed on Q'' rather than U_m in the assessment of spray cooling performance.

The nozzle's orifice-to-surface distance is perhaps one of the most elusive parameters in the spray cooling literature. Aside from ensuring fully developed breakup of the spray droplets, this distance has a strong bearing on the magnitude and spatial distribution of volumetric flux. Because many past studies either ignored specifying this distance for each spray test or used the same orifice-to-surface distance for different nozzles, it is difficult to utilize such data in the development of generalized heat transfer models or correlations. Mudawar and Estes [7] recommended a systematic yet simple method for specifying the orifice-to-surface distance in order to obtain useful spray data. They proved that to maximize critical heat flux (CHF) in order to broaden the cooling heat flux range for a spray nozzle, the orifice-to-surface distance must be configured such that the spray impact area just inscribe the surface of the device. An orifice-to-surface distance that is shorter than required by this criterion would concentrate the coolant in a small central portion of the surface, while a larger distance would cause part of the coolant's flow rate to be wasted outside the surface.

Another parameter that influences spray cooling performance is subcooling. Supplying the coolant at a temperature far lower than the saturation temperature allows the spray cooling system to utilize sensible heat content of the droplets in addition to latent heat.

The influence of the aforementioned parameters is greatly complicated by two additional influences that are dictated by geometrical and packaging requirements: spray inclination and spray overlap. Spray nozzles are sometimes tilted relative to the normal to the surface in order to reduce both orifice-to-surface distance and overall volume of a spray-cooling module. Spray inclination has a profound influence on the distribution of droplets across the surface and, hence, cooling performance. Spray overlap is used in cooling modules that house a single large heat-dissipating area or multiple heat-dissipating areas. Such overlap increases volumetric flux in the overlap region and, therefore, influences cooling performance.

Clearly, designing a spray cooling system for electronics cooling is a complicated endeavor. This paper aims to consolidate existing literature as well as provide new relations and methodologies for designing a spray-cooling module. A comprehensive database for FC-72, FC-87, FC-77, PF-5052, and water full-cone pressure sprays that has been amassed by the authors and their coworkers is used to explore the complex influences of individual spray parameters on cooling performance. Table I provides key thermophysical properties for all these coolants. The database includes variations of nozzle, flow rate, subcooling and orientation. A new CHF correlation

TABLE I
THERMOPHYSICAL PROPERTIES OF DIFFERENT FLUIDS AT ONE ATMOSPHERE

Properties at saturation temperature							
Fluid	T_{sat} (°C)	ρ_f (kg/m^3)	ρ_g (kg/m^3)	σ x 10^3 (N/m)	h_{fg} (kJ/kg)	$c_{p,f}$ (J/kg.K)	μ_f x 10^6 (N.s/m^2)
Water	100	957.9	0.569	58.9	2257	4217	279.0
FC-77	97	1600.0	12.66	8.23	78.75	1164	454.0
FC-72	56	1616.4	13.72	9.37	84.20	1098	440.6
PF-5052	50	1642.5	12.00	13.0	104.7	1092	517.2
Properties at 23 °C							
Fluid	T_f (°C)	ρ_f (kg/m^3)	ρ_g (kg/m^3)	σ x 10^3 (N/m)	h_{fg} (kJ/kg)	$c_{p,f}$ (J/kg.K)	μ_f x 10^6 (N.s/m^2)
Water	23	998.0	0.019	72.8	2449	4181	959.0
FC-77	23	1782.0	-	13.93	-	1050	1329
FC-72	23	1684.0	3.95	12.2	93.65	1045	662.6
PF-5052	23	1715.1	-	13.0	-	1050	703.2

is developed that accounts for variations in all these parameters, including spray orientation. Also presented is a new methodology for assessing the influence of overlap between neighboring sprays on cooling performance.

II. EXPERIMENTAL METHODS

A. Test Heater

The experimental work described in this paper includes studies of normal upward-facing PF-5052 sprays, normal and inclined downward-facing PF-5052 sprays, and normal downward-facing FC-77 sprays. The same test heater and two-phase flow loop were used in all three studies; however, different spray chambers and spray nozzle positioning hardware were required to accommodate the different spray orientations.

The primary purpose of the test heater is to simulate high-flux heat dissipation from an electronic device. As shown in Fig. 1(a), the main part of the test heater is an oxygen-free copper block that has an enlarged bottom to accept nine cartridge heaters, and is tapered in two steps to the top 1.0×1.0 cm^2 test surface area. The top portion of the copper block is inserted into a thick insulating G-7 fiberglass plastic plate. The bottom portion of the copper block is wrapped with a fiberglass insulating blanket. One-dimensional heat conduction is assumed between a type-K thermocouple embedded 1.27 mm below the test surface and the test surface itself to determine the surface temperature. The test surface protrudes slightly above the G-7 insulation to prevent liquid accumulation on the surface for downward-facing sprays. Fig. 1(b) shows a dimensioned top view of the copper block.

B. Spray Chambers

Two separate chambers were used in this study. Fig. 2(a) shows a schematic of the first chamber that is used with upward-facing PF-5052 sprays. The test heater is mounted atop the test chamber, and the spray nozzle positioned relative to the test surface with aid of a micrometer translation stage. The vapor generated by droplet evaporation accumulates in the top region of the test chamber, from where it is bled through two separate outlets to an external condenser. Any unevaporated liquid accumulates at the bottom of the test chamber before draining into an external reservoir beneath. The chamber is made of G-10 fiberglass plastic and fitted in the front and back with transparent polycarbonate plastic walls. A pressure transducer is connected to the chamber's sidewall to measure the spray chamber's pressure. The temperature of vapor surrounding the spray is measured by a thermocouple that is inserted into the chamber. The coolant tube leading to the nozzle is fitted with a second pressure transducer and another temperature sensor to measure the coolant's flow conditions upstream of the nozzle.

Normal downward-facing FC-77 sprays and inclined PF-5052 sprays are tested in a larger spray chamber that is designed to accommodate a three-degree-of-freedom nozzle positioning system. This larger spray chamber features essentially the same instrumentation as the smaller chamber except for mounting the test heater at the bottom of the chamber instead of atop. Fig. 2(a) depicts the nozzle positioning system of the larger chamber. The vertical translation stage of the positioning system, which is mounted on two vertical rods, is used to adjust the orifice-to-surface distance with the aid of an external micrometer. The horizontal position of the nozzle's

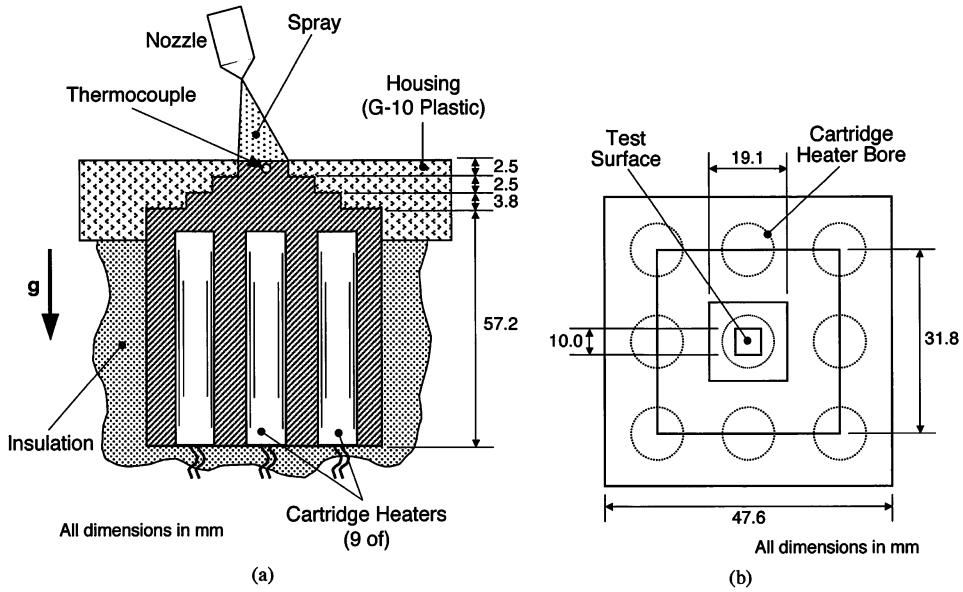

Fig. 1. (a) Sectional view of heater assembly. (b) Top view of copper block.

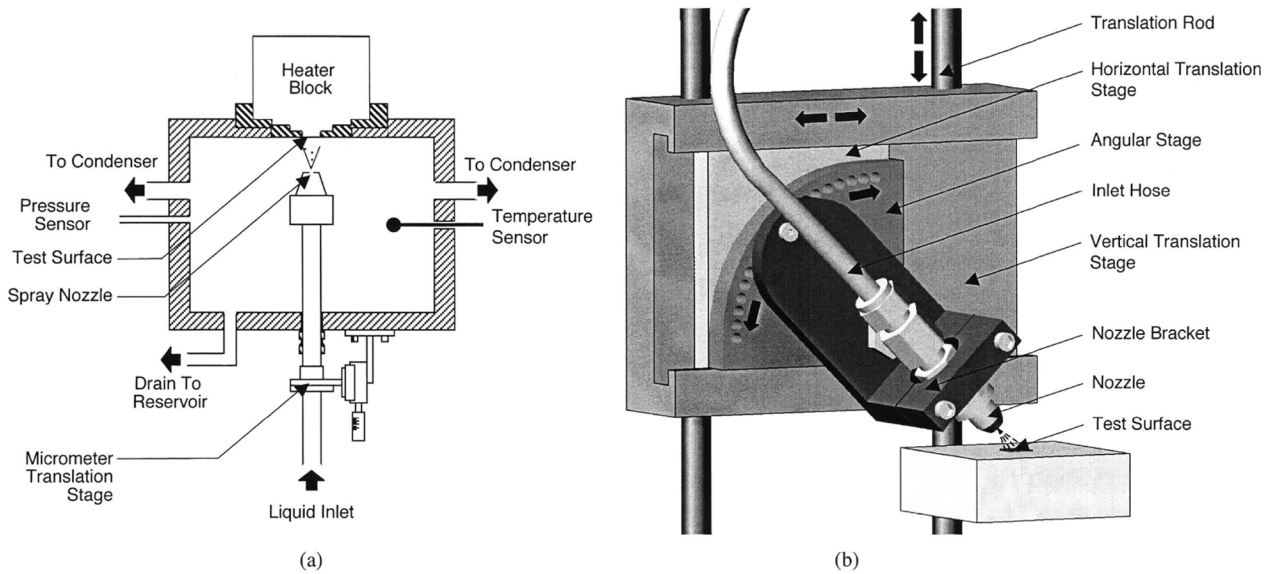

Fig. 2. (a) Schematic of spray chamber with upward spray orientation. (b) Nozzle positioning system used in downward and inclined spray orientations.

orifice relative to the test surface is adjusted using a horizontal translation stage that slides through rectangular grooves in the vertical stage. An angular stage having holes that span 0° to 90° is attached to the horizontal stage. The nozzle is attached to a bracket that is connected to the angular stage. One end of this bracket is pivoted at a fixed point on the angular stage while the other end is fixed to one hole of the angular stage to set the desired nozzle orientation relative to the test surface.

C. Two-Phase Flow Loop

Fig. 3 shows a schematic of the two-phase flow loop that is used to condition the coolant to the desired pressure, temperature, and flow rate at the nozzle inlet. The bulk of the coolant resides in a reservoir situated immediately above a deareation chamber. An immersion heater in the deaeration chamber serves two different purposes. Before the tests, this heater is used to bring the coolant to a vigorous boil to help remove any dissolved gases while, during the tests, it preheats the coolant to the desired temperature. Two variable-speed centrifugal pumps are connected in parallel to achieve a broad range of coolant flow rates. The pumped coolant passes through a filter followed by one of two rotameters before passing through a high-capacity air-cooled heat exchanger. This heat exchanger provides the desired degree of subcooling in the coolant entering the spray nozzle. Inside the spray chamber, the spent fluid is separated by buoyancy. The unevaporated liquid drains into the reservoir while the vapor is routed to an elevated condenser where it condenses back into liquid that drips down back into the reservoir.

D. Operating Procedure

Tests are initiated by positioning the spray nozzle relative to the test surface inside the spray chamber. For normal sprays,

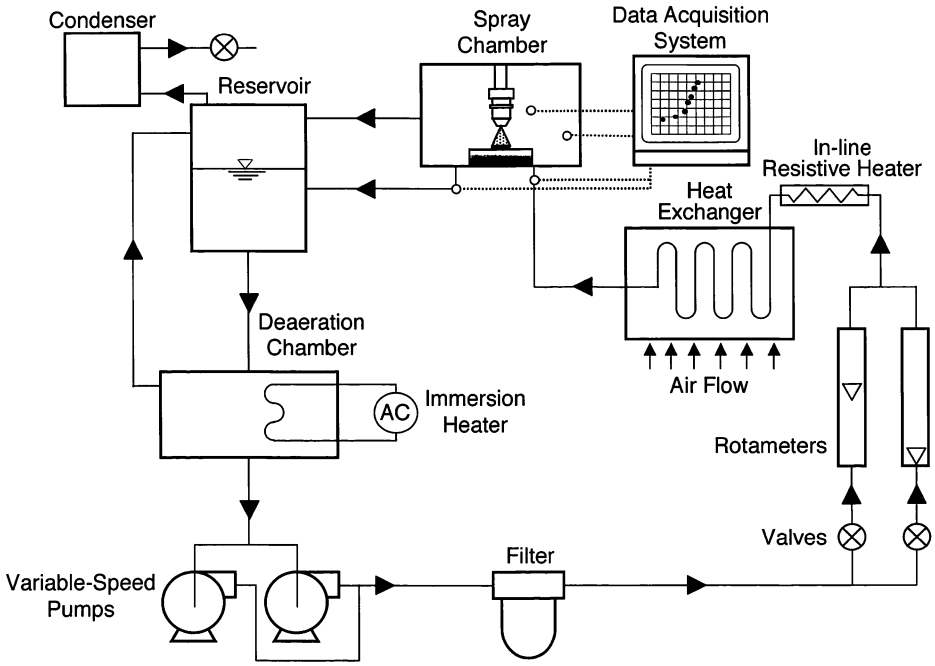

Fig. 3. Two-phase flow loop.

only the orifice-to-surface distance has to be adjusted. The spray chamber is then carefully sealed.

Deaeration is initiated by bringing the coolant in the deaeration chamber to a vigorous boil for 30 min. A mixture of the coolant's vapor and dissolved noncondensable gases rises to the condenser, where the coolant condenses and is recovered by dripping into the reservoir while the noncondensible gases are purged to the ambient. The pumps are then turned on and the deareation process continued for an additional 30 min as the coolant is circulated through the loop. The condenser vent is then closed to seal the system from the ambient.

Tests are initiated by modulating the speed of the two pumps to achieve the desired flow rate. Pressure in the spray chamber is maintained at atmospheric level while the coolant's temperature at the nozzle inlet is modulated to the desired subcooling level with the aid of the immersion heater inside the deaeration chamber and/or the air-cooled heat exchanger. Once the desired operating conditions are achieved, electrical power is supplied to the test heater in small increments. Data are recorded between increments after the heater reaches steady state temperature. This process is repeated until an unsteady rise in the heater's temperature following the last power increment signals the commencement of CHF, at which point the electrical power is turned off.

It is important to emphasize that all tests of the present study adhere to the geometrical requirement recommended by Mudawar and Estes [7] to maximize CHF. For normal upward-facing or downward-facing sprays, the orifice-to-surface distance is adjusted such that the spray impact area just inscribes the square test surface, i.e., with the diameter of the impact area equal to the length of the test heater. Since the impact area of an inclined spray is an ellipse rather than a circle, the orifice-to-surface distance for an inclined spray is adjusted such that the major axis of the impact ellipse just inscribes the square test surface.

TABLE II
CHARACTERISTICS OF SPRAY NOZZLES USED IN PRESENT STUDY

Nozzle	Orifice Diameter d_o (mm)	Spray Angle θ (°)	Sauter Mean Diameter $d_{32} \times 10^6$ (m)	Volumetric Flow Rate $Q \times 10^6$ ($m^3 s^{-1}$)
1	0.762	55.8	111 - 123	3.33 – 4.33
2	1.19	46.4	160 - 179	4.93 - 13.5
3	1.70	48.5	189 - 249	12.5 – 23.9

Three Unijet full-cone pressure spray nozzles made by Spraying Systems Company are used in this study. Table II provides key geometrical and flow parameters of these nozzles.

Uncertainties in the pressure, flow rate, and temperature measurements are estimated at less than 0.5%, 1.0%, and ± 0.2°C, respectively. Heat loss is estimated at less than 2% of the electrical power input to the test heater [8].

III. FLOW VISUALIZATION OF SPRAYS

High-speed video analysis was conducted to capture the impact behavior of sprays for different spray orientations. Representative video segments were recorded by a FASTCAM-Ultima APX FM camera at 6000 fps with 512×512 resolution and a shutter speed of 1/6000 s.

Fig. 4 shows snapshots from video records for nozzle 1 sprays at a relatively low flow rate of 4.5×10^{-7} m^3/s and inclination angles of 0°, 40°, and 55°. This flow rate is within the operating range recommended by the manufacturer for this particular nozzle. The images in Fig. 4 were captured at 90%–95% of CHF.

As indicated in the previous section, the impact area for an inclined spray is an ellipse. CHF for inclined sprays is maximized by setting the orifice-to-surface distance such that the

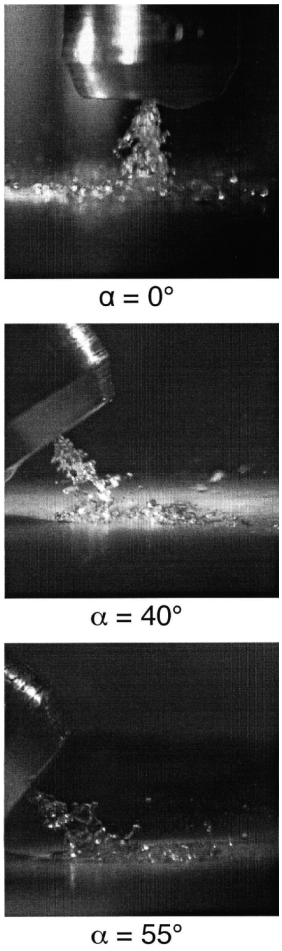

Fig. 4. High-speed video images of nozzle 1 sprays at a low flow rate of 4.5×10^{-7} m^3/s for pre-CHF conditions.

major axis of the impact ellipse just inscribe the square test surface. This explains why the orifice-to-surface distance in Fig. 4 is decreased for increasing spray inclinations.

Fig. 4 shows normal impact ($\alpha = 0°$) produces fairly symmetrical droplet breakup and distribution across the test surface. On the other hand, droplets in an inclined spray can have vastly different travel distances before impact. There is also a tendency for droplets to form a liquid film that travels along the test surface, especially for steep inclinations.

Video analysis is especially effective at pinpointing the location across the test surface where CHF commences. Mudawar and Estes [7] proved CHF commences at surface locations receiving the weakest volumetric flux. For normal full cone sprays, they showed volumetric flux is weakest along the periphery of the spray impact area. For inclined sprays, one would expect volumetric flux to be weakest at the point farthest from the nozzle orifice. However, the video analysis revealed that, while the endpoint of the major axis farthest from the orifice does receive the least spray liquid by direct impact (albeit at an incline), the same location receives additional liquid in the form of a film that flows along the test surface. Hence, the location of least volumetric flux is that which does not benefit from the additional film flow. Two such surface locations are the endpoints of the minor axis of the impact ellipse. These

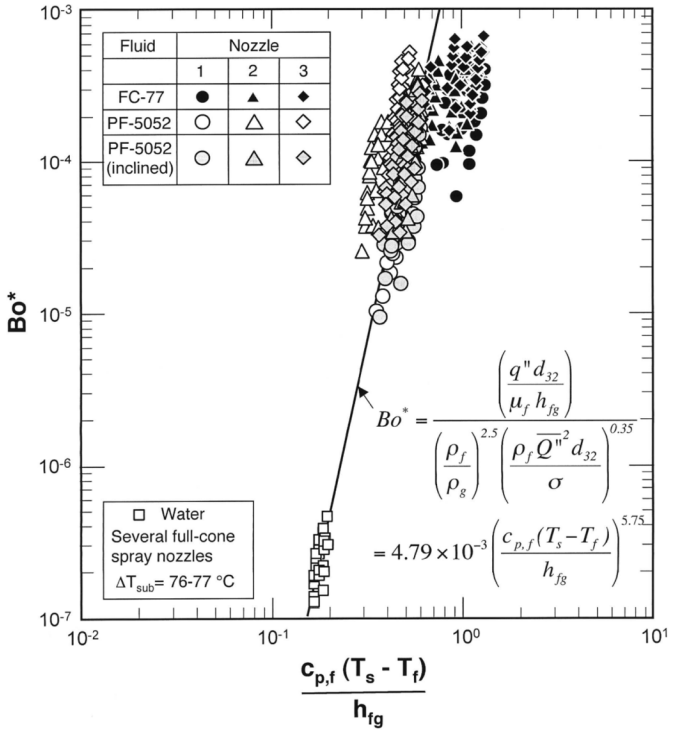

Fig. 5. Nucleate boiling correlation for upward-facing, downward-facing and inclined PF-5052 sprays, downward-facing FC-77 sprays, and downward-facing water sprays.

endpoints are therefore where CHF commences for an inclined spray. Additional details of the flow visualization study for different spray inclinations and flow rates are available in [13], [14].

IV. Experimental Results and Design Relations and Models

A. Nucleate Boiling Heat Transfer Coefficient

Recently, Rybicki and Mudawar [8] combined their normal upward-facing PF-5052 spray data with the downward-oriented water spray data of Mudawar and Valentine [5] to derive the following nucleate boiling correlation

$$\frac{q'' d_{32}}{\mu_f h_{fg}} = 4.79 \times 10^{-3} \left(\frac{\rho_f}{\rho_g}\right)^{2.5} \times \left(\frac{\rho_f \bar{Q}''^2 d_{32}}{\sigma}\right)^{0.35} \left(\frac{c_{p,f}(T_s - T_f)}{h_{fg}}\right)^{5.75}. \quad (1)$$

Fig. 5 shows the present authors' new inclined-spray PF-5052 data and normal downward-facing FC-77 data are fairly well predicted by the same correlation. Equation (1) indicates increasing the mean volumetric flux enhances heat transfer in the nucleate boiling region. Aside from simply increasing the coolant's flow rate, the mean volumetric flux may be increased by using overlapping sprays. This important issue will be discussed later in this paper.

B. Critical Heat Flux for Normal and Inclined Sprays

Mudawar and Estes [7] proved experimentally that CHF in a normal full-cone spray is initiated at the locations of weakest

volumetric flux along the test surface. They developed a uniform point source model for the spray in which the total flow rate Q is uniformly distributed over any spherical surface centered at the orifice. The uniform volumetric flux distribution along a spherical surface whose radius equals the orifice-to-surface distance is projected into a nonuniform distribution along the flat test surface, where volumetric flux decreases away from the center of the surface. Therefore, volumetric flux for a spray that just inscribes the test surface (i.e., with an impact diameter that equals the width of the test surface) is weakest along the outer edge of the impact area. This edge is the locus of points where CHF is initiated before spreading inwards towards the center. Based on data for normal downward-facing FC-72 and FC-87 sprays, as well as earlier data for normal downward-facing water sprays [5], Estes and Mudawar [6], [7] developed the following correlation for point-based or local CHF along the outer edge of the impact area

$$\frac{q''_{m,p}}{\rho_g h_{fg} Q''} = 2.3 \left(\frac{\rho_f}{\rho_g}\right)^{0.3} \left(\frac{\rho_f Q''^2 d_{32}}{\sigma}\right)^{-0.35} \times \left(1 + 0.0019 \frac{\rho_f c_{p,f} \Delta T_{\text{sub}}}{\rho_g h_{fg}}\right). \quad (2)$$

This same correlation was recently validated by Rybicki and Mudawar [8] for normal upward-facing PF-5052 sprays. Notice that Q'' in (2) is the local volumetric flux along the outer periphery of the circular spray impact area, which is given by [7]

$$Q'' = \frac{2Q}{\pi L^2}[1 + \cos(\theta/2)]\cos(\theta/2). \quad (3)$$

The Sauter mean diameter d_{32} in (2) is related to the spray's Weber and Reynolds numbers based on the nozzle's orifice diameter [6]

$$\frac{d_{32}}{d_o} = 3.67 \left[\text{We}_{d_o}^{1/2} \text{Re}_{d_o}\right]^{-0.259}. \quad (4)$$

Notice that the influence of volumetric flux on Sauter mean diameter is implicit in (4), where both the nozzle Weber number We_{do} and the nozzle Reynolds number Re_{do} are defined with respect to nozzle pressure drop ΔP. For pressure spray nozzles, ΔP is proportional to Q^2, adjusted with a flow coefficient that is nozzle specific. Thus, (4) proves that, for a given nozzle and ΔP, d_{32} is related to total nozzle flow rate and, therefore, volumetric flux.

The authors of the present study developed a theoretical scheme for adapting (2) to inclined sprays [13], [14], which was validated with PF-5052 spray data. Fig. 6 shows a schematic of an inclined spray whose orifice-to-surface distance is adjusted such that the major axis of the impact spray just inscribe the square test surface in order to maximize CHF. Shown in Fig. 6 is the detailed nomenclature used in modeling the effects of spray orientation on CHF. As explained earlier, the weakest volumetric flux for an inclined spray occurs at the endpoints of the minor axis of the impact area rather than the endpoint of the major axis farthest from the orifice. The original Estes and Mudawar [6] CHF correlation was modified with geometrical functions that account for spray inclination effects.

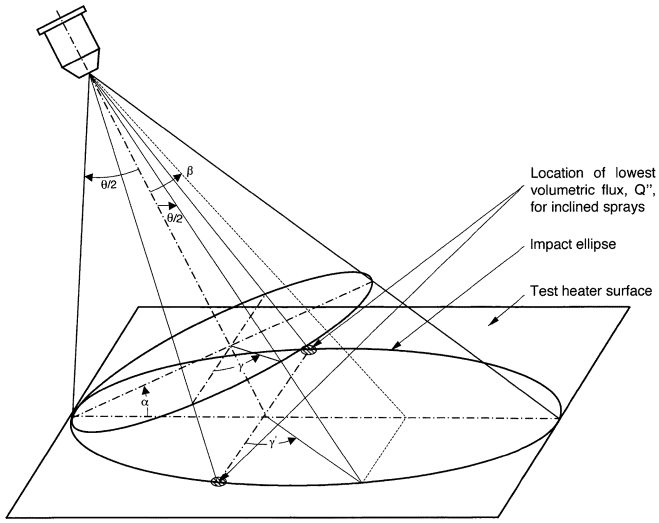

Fig. 6. Nomenclature for angles used in inclined spray model.

One limitation of the spray databases used by Estes and Mudawar [6], [7] to develop (2) is the relatively small range of subcooling. Recently, the authors of the present study developed a new extensive CHF database for normal downward-facing FC-77 sprays corresponding to a much broader range of subcooling, 22 °C–77 °C. They determined that the effect of subcooling is more pronounced than predicted by (2), and recommended increasing the magnitude of the constant in the subcooling term from 0.0019 to 0.0050.

Therefore, it is possible to develop a new universal CHF correlation that combines the inclination functions developed earlier [14] and the corrected subcooling constant. This correlation is presented in terms of the measured CHF q''_m and volumetric flux averaged over the spray's impact area $\bar{Q}''$

$$\frac{q''_m}{\rho_g h_{fg} \bar{Q}''} = 2.3 \left(\frac{\rho_f}{\rho_g}\right)^{0.3} \left(\frac{\rho_f \bar{Q}''^2 d_{32}}{\sigma}\right)^{-0.35} \times \left(1 + 0.0050 \frac{\rho_f c_{p,f} \Delta T_{\text{sub}}}{\rho_g h_{fg}}\right) \left(\frac{f_1^{0.30}}{f_2}\right). \quad (5)$$

where

$$q''_m = \frac{P_W}{L^2} \quad (6)$$

$$\bar{Q}'' = \frac{Q}{\frac{\pi}{4} L^2 \cos\alpha \sqrt{1 - \tan^2\alpha \tan^2(\theta/2)}} \quad (7)$$

$$f_1 = \frac{Q''}{\bar{Q}''} = \frac{1}{8}\left(\frac{L}{H}\right)^2 \times \frac{\cos\alpha \sqrt{1 - \tan^2\alpha \tan^2(\theta/2)}}{1 - \cos(\theta/2)} \frac{dA'}{dA} \quad (8)$$

and

$$f_2 = \frac{q''_{m,p}}{q''_m} = \frac{1}{\left[\frac{\pi}{4}\cos\alpha \sqrt{1 - \tan^2\alpha \tan^2(\theta/2)}\right]} \quad (9)$$

and α in the spray's inclination angle measured between the axis of the spray and the normal to the test surface. The term *dA'/dA* in (8) is the ratio of an infinitesimal area of a spherical surface that is centered at the orifice to the projection of the same area

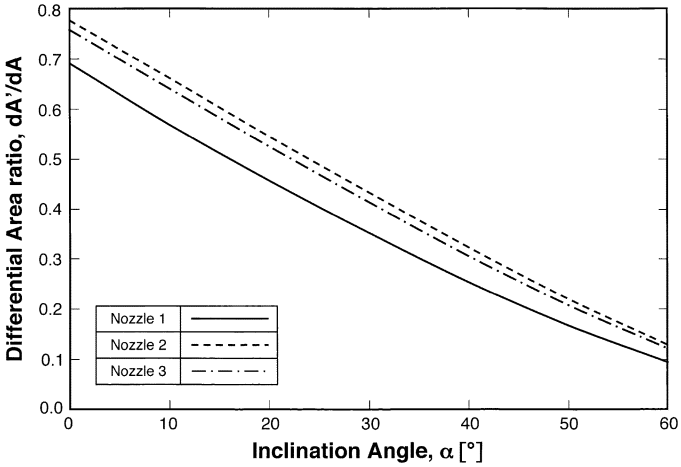

Fig. 7. Variation of differential area ratio corresponding to end points of minor axis of impact ellipse with inclination angle for three nozzles [13].

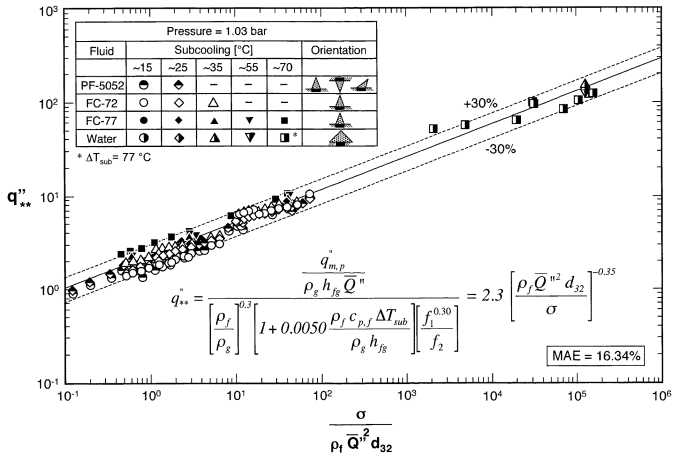

Fig. 8. Correlation of CHF data for different nozzles, fluids, flow rates, subcoolings, and orientations.

onto the test surface [13]; this ratio is evaluated numerically at the endpoints of the minor axis. Notice that for a normal spray, f_1 is simply Q'', given by (3), divided by $Q/(\pi L^2/4)$. For inclined sprays, Fig. 7 shows numerically calculated values for *dA'/dA* for different inclination angles for each of the three nozzles tested. Fig. 8 shows the new CHF correlation predicts data for different nozzles, flow rates, subcoolings, and inclination angles with a mean absolute error (MAE) of 16.34%.

V. Spray Overlap

Overlapping sprays are used in electronics cooling systems to cool a single relatively large device or multiple devices inside a single cooling module. Using overlapping sprays is based on the notion that the overlap region both increases mean volumetric flux as well as helps maintain a more uniform spatial distribution of volumetric flux and, therefore, smaller temperature gradients across the surface the electronic device. However, no models presently exist to guide the design of overlapping sprays. The method described here is the first attempt at providing quantitative means for assessing the influence of spray overlap for normal sprays.

A clear distinction must be made regarding the influence of spray overlap on heat transfer in the nucleate boiling region versus CHF. Many possible overlap patterns exist, so a simple configuration is discussed here to demonstrate how the impact of spray overlap can be tackled. Consider the case of two sprays that are used to cool two square heaters situated side-by-side, or a single large rectangular heater. Fig. 9 shows two different cooling options. The first involves inscribing the impact area of each spray within the boundaries of each square heater. The second involves some spray overlap. While some collision might take place among droplets emanating from the two sprays, the most significant impact of the spray overlap is greater volumetric flux within the overlap region; the local volumetric flux is unaffected elsewhere across the surfaces of the two heaters. Since CHF is dictated by the magnitude and location of weakest volumetric flux, it will occur along the outer edge for each of the patterns depicted in Fig. 9. Therefore, CHF for the overlapping pattern is unaffected by the overlap since CHF is initiated in the weakest unoverlapping corner regions for each of the heaters. However, the overlap increases both the local volumetric flux in the overlap region and the mean volumetric flux $\bar{Q}''$ for each heater. Equation (1) shows the overlap should enhance heat transfer in the nucleate boiling region for each heater. Therefore, the task of assessing this enhancement effect consists of estimating $\bar{Q}''$ for overlapping sprays and simply introducing this value in (1) to determine the relationship between heat flux and surface temperature in the nucleate boiling region. It is important to indicate that the spray overlap model below is intended for identical sprays. The reason behind retaining subscripts 1 and 2 in the model derivation is to track the source of fluid in the overlap region.

Estimating $\bar{Q}''$ for heater 1 consists of first determining the increase in coolant flow rate Q_{ol} caused by coolant from spray 2 that impacts heater 1 in the overlap area A_{ol}. Different total flow rates are assumed for heaters 1 and 2 to provide generalized results

$$Q_{ol} = \int \int_{A_{ol}} Q_2'' \, dA, \tag{10}$$

where, from [7]

$$Q_2'' = \frac{Q_2}{2\pi H^2[1-\cos(\theta/2)]} \, 1\left[1 + \left(\frac{r}{H}\right)^2\right]^{3/2}. \tag{11}$$

Substituting the above expression in (10) and integrating over the overlap region yield

$$Q_{ol} = \frac{Q_2}{2\pi H^2 \left[1-\cos(\theta/2)\right]} \, 2 \times \int_{\xi=0}^{\phi} \int_{r=\frac{R\cos\phi}{\cos\xi}}^{r=R} \frac{1}{\left[1+\left(\frac{r}{H}\right)^2\right]^{3/2}} \, r \, d\xi \, dr \tag{12}$$

where

$$\phi = \cos^{-1}\left(\frac{L}{2R}\right). \tag{13}$$

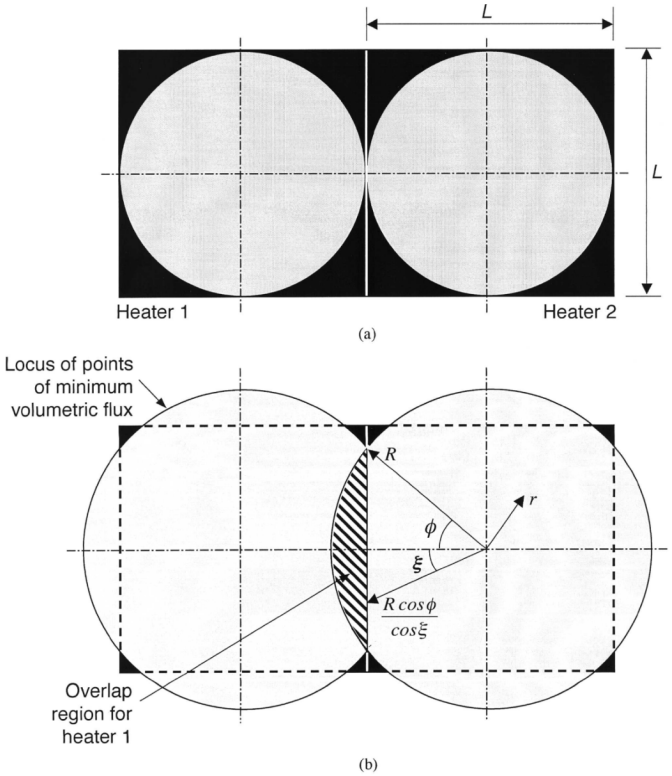

Fig. 9. Two adjacent square heaters impacted by two sprays that are configured (a) for maximum CHF (diameter of impact area equal heater width) and (b) with overlap to enhance nucleate boiling heat transfer coefficient by increasing mean volumetric flux.

Equation (12) can be simplified further into

$$Q_{ol} = \frac{Q_2}{\pi[1-\cos(\theta/2)]} \times \int_{\xi=0}^{\phi} \left[\frac{-1}{\sqrt{\left(1+\left(\frac{R}{H}\right)^2\right)}} + \frac{1}{\sqrt{\left[1+\left(\frac{R\cos\phi}{H\cos\xi}\right)^2\right]}} \right] d\xi = \frac{Q_2}{\pi[1-\cos(\theta/2)]} f_o. \quad (14)$$

The integral function, f_o, in (14) is solved numerically for different values of R/H and ϕ as shown in Fig. 10. Notice how f_o increases with increasing ϕ due to the increased size of the overlap area. f_o also increases with increasing R/H up to $R/H \sim 1.3$ but decreases for larger values as the coolant flow from spray 2 begins to be wasted outside of heater 1.

The mean volumetric flux for heater 1 can be determined as follows. First, the total flow rate for spray 1 fluid is Q_1, of which the portion

$$\frac{4\,Q_1}{\pi[1-\cos(\theta/2)]} f_o$$

corresponding to four times the overlap area fails to impact heater 1. The portion of the spray 2 flow rate that impacts heater 1 is

$$\frac{Q_2}{\pi[1-\cos(\theta/2)]} f_o.$$

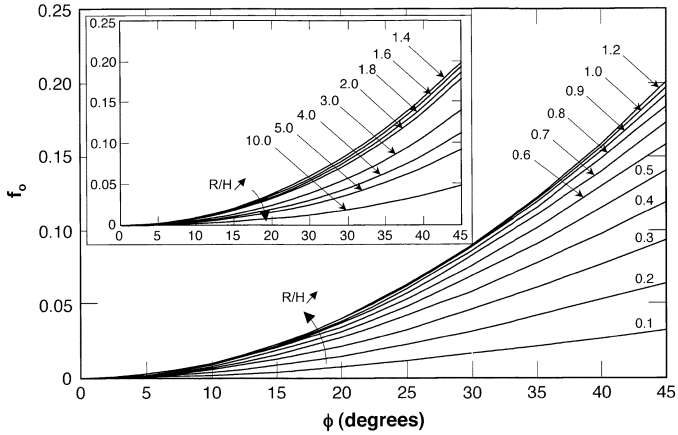

Fig. 10. Variation of function f_o for different f and R/H values.

The total flow rate from sprays 1 and 2 that impacts heater 1 is

$$Q_1 - \frac{4Q_1}{\pi[1-\cos(\theta/2)]} f_o + \frac{Q_2}{\pi[1-\cos(\theta/2)]} f_o = Q_1 \left[1 - \frac{Q_1}{\pi[1-\cos(\theta/2)]} f_o(4 - Q_2/Q_1)\right]. \quad (15)$$

The average volumetric flux impacting heater 1 is obtained by dividing the above expression by the spray impact area for spray 1

$$\bar{Q}_1 = \frac{Q_1}{\left(\frac{\pi D^2}{4}\right)} \left[1 - \frac{Q_1}{\pi[1-\cos(\theta/2)]} f_o(4 - Q_2/Q_1)\right] = \frac{Q_1}{\left(\frac{\pi D^2}{4}\right)} \left[1 - \frac{3\,Q_1\,f_o}{\pi[1-\cos(\theta/2)]}\right]. \quad (16)$$

This average volumetric flux can be used in (1) to determine the nucleate boiling characteristics for heater 1.

As mentioned earlier, several overlap patterns are possible. The technique described above for two overlapping sprays shows how the models and correlations of single sprays can be used to assess the influence of spray overlap.

VI. Conclusion

This paper summarizes the process of systematically predicting the two-phase cooling performance of full-cone sprays. Tests with several coolants (water, FC-72, FC-77, FC-87, and PF-5052) were used to generate a comprehensive database for different nozzles, flow rates, subcooling, and orientations. A new CHF correlation is recommended and a scheme for assessing the influence of spray overlap on cooling performance described. Key conclusions from the study are as follows.

1) CHF for a normal spray is initiated along the outer periphery of the impact area corresponding to weakest volumetric flux. CHF for a normal spray is maximized when the orifice-to-surface distance is such that the spray impact area just inscribe the square surface of the heating-dissipating device. The impact area of an inclined spray is an ellipse and CHF is maximized with an orifice-to-surface distance that just inscribes the major axis within the square surface. While the farthest downstream endpoint of the major axis receives the least volumetric flux from direct

liquid impact, liquid flow rate in this region is increased by a liquid film that flows along the surface towards the same endpoint. This film causes the least volumetric flux to commence at the endpoints of the minor axis and CHF commences at these two points.

2) A previous CHF correlation for normal sprays is modified for both inclination and subcooling effects. A new universal user-friendly CHF correlation is recommended that shows excellent predictive capability for the entire spray database.
3) A systematic scheme is presented to assess the influence of spray overlap on cooling performance. Because CHF is dictated by the location and magnitude of weakest volumetric flux, overlap may not influence CHF for several overlap patterns. However, by increasing the mean volumetric flux, overlap can have appreciable influence on the nucleate boiling region. A theoretical scheme is presented to determine the mean volumetric flux for overlapping sprays.

REFERENCES

[1] I. Mudawar, "Assessment of high-heat-flux thermal management schemes," *IEEE Trans. Compon. Packag Technol.*, vol. 24, no. 2, pp. 122–141, Jun. 2001.

[2] S. Toda, "A study in mist cooling (1st report: Investigation of mist cooling)," *Trans. JSME*, vol. 38, pp. 581–588, 1972.

[3] M. Monde, "Critical heat flux in saturated forced convection boiling on a heated disk with impinging droplets," *Trans. JSME*, vol. 8, pp. 54–64, 1979.

[4] S. Toda and H. Uchida, "Study of liquid film cooling with evaporation and boiling," *Trans. JSME*, vol. 2, pp. 44–62, 1973.

[5] I. Mudawar and W. S. Valentine, "Determination of the local quench curve for spray-cooled metallic surfaces," *J. Heat Treating*, vol. 7, pp. 107–121, 1989.

[6] K. A. Estes and I. Mudawar, "Correlation of Sauter mean diameter and critical heat flux for spray cooling of small surfaces," *Int. J. Heat Mass Transfer*, vol. 38, pp. 2985–2996, 1995.

[7] I. Mudawar and K. A. Estes, "Optimizing and predicting CHF in spray cooling of a square surface," *J. Heat Transfer*, vol. 118, pp. 672–680, 1996.

[8] J. R. Rybicki and I. Mudawar, "Single-phase and two-phase cooling characteristics of upward-facing and downward-facing sprays," *Int. J. Heat Mass Transfer*, vol. 49, pp. 5–16, 2006.

[9] C. S. K. Cho and K. Wu, "Comparison of burnout characteristics in jet impingement cooling and spray cooling," in *Proc. Nat. Heat Transfer Conf.*, Houston, TX, 1988, vol. 1, pp. 561–567.

[10] R.-H. Chen, L. C. Chow, and J. E. Navedo, "Effects of spray characteristics on critical heat flux in subcooled water spray cooling," *Int. J. Heat Mass Transfer*, vol. 45, pp. 4033–4043, 2002.

[11] E. A. Silk, J. Kim, and K. Kiger, "Effect of spray cooling trajectory on heat flux for a straight finned enhanced surface," in *Proc. Nat. Heat Transfer Summer Conf.*, San Francisco, CA, 2005, Paper HT2005-72634.

[12] B. Q. Li, T. Cader, J. Schwarzkopf, K. Okamoto, and B. Ramaprian, "Spray angle effect during spray cooling of microelectronics: Experimental measurements and comparison with inverse calculations," *Appl. Thermal Eng.*, vol. 26, pp. 1788–1795, 2006.

[13] M. Visaria and I. Mudawar, "Theoretical and experimental study of the effects of spray inclination on two-phase spray cooling and critical heat flux," *Int. J. Heat Mass Transfer*, vol. 51, pp. 2398–2410, 2008.

[14] M. Visaria and I. Mudawar, "A systematic approach to predicting critical heat flux for inclined sprays," *ASME J. Electron. Packag.*, vol. 129, pp. 452–459, 2007.

[15] L. Lin and R. Ponnappan, "Heat transfer characteristics of spray cooling in a closed loop," *Int. J. Heat Mass Transfer*, vol. 46, pp. 3737–3746, 2003.

[16] A. G. Pautsch and T. A. Shedd, "Spray impingement cooling with single- and multiple-nozzle arrays. Part I: Heat transfer data using FC-72," *Int. J. Heat Mass Transfer*, vol. 48, pp. 3167–3175, 2005.

[17] D. D. Hall and I. Mudawar, "Experimental and numerical study of quenching complex-shaped metallic alloys with multiple, overlapping sprays," *Int. J. Heat Mass Transfer*, vol. 38, pp. 1201–1216, 1995.

Milan Visaria received the B.E. degree from Mumbai University, Mumbai, India, in 2004 and the M.S. degree from Purdue University, West Lafayette, IN, in 2006. He is currently pursuing the Ph.D. degree in the School of Mechanical Engineering at Purdue University. His M.S. work involved the study of two-phase spray cooling for electronics applications at the Boiling and Two-Phase Flow Laboratory (BPTFL).

He currently works at the Purdue University Hydrogen Systems Laboratory and BTPFL focusing on the development of a new class of heat exchangers for the storage of hydrogen in automobiles.

Issam Mudawar received the M.S. and Ph.D. degrees from the Massachusetts Institute of Technology, Cambridge, in 1980 and 1984, respectively. His graduate work involved magnetohydrodynamic (MHD) energy conversion and phase-change water cooling of turbine blades.

He joined the School of Mechanical Engineering, Purdue University, West Lafayette, IN, in 1984, where he established, and became Director of, the Boiling and Two-Phase Flow Laboratory (BTPFL) and Purdue University International Electronic Alliance (PUIECA). His work has been focused on phase change processes, thermal management of electronic and aerospace devices, intelligent materials processing, hydrogen storage, high-Mach turbine engines, and nuclear reactor safety. His theoretical and experimental research encompasses sensible and evaporative heating of thin films, pool boiling, flow boiling, jet-impingement cooling, spray cooling, microchannel heat sinks, heat transfer enhancement, heat transfer in rotating systems, critical heat flux, and capillary pumped flows. He is also President of Mudawar Thermal Systems, Inc., a firm that is dedicated to the development of thermal management solutions.

Prof. Mudawar received several awards for his research accomplishments, including Best Paper Award in Electronic Cooling at the 1988 National Heat Transfer Conference, Best Paper Award in Thermal Management at the 1992 ASME/JSME Joint Conference on Electronic Packaging, the *Journal of Electronic Packaging* Outstanding Paper of the Year Award for 1995, and the Best Paper Award in Thermal Management at ITherm 2008. He also received several awards for excellence in teaching and service to Purdue students and their organizations, including the Solberg Award for Best Teacher in School of Mechanical Engineering (1987, 1992, 1996, 2004), the Charles Murphy Award for Best Teacher at Purdue University (1997), and the National Society of Black Engineers Professor of the Year Award (1985, 1987). He was named Fellow of the American Society of Mechanical Engineers (ASME) in 1998.